Suprathreshold contrast response in normal and anomalous trichromats

KENNETH KNOBLAUCH,[1,2,*] BRENNAN MARSH-ARMSTRONG,[3] AND JOHN S. WERNER [3]

[1] *Univ Lyon, Université Claude Bernard Lyon 1, Inserm, Stem Cell and Brain Research Institute U1208, 69500 Bron, France*
[2] *National Centre for Optics, Vision and Eye Care, Faculty of Health and Social Sciences, University of South-Eastern Norway, Hasbergsvei 36, 3616 Kongsberg, Norway*
[3] *Vision Science and Advanced Retinal Imaging Laboratory, Department of Ophthalmology and Vision Science, University of California, Davis, USA*
[*] *ken.knoblauch@inserm.fr*
https://www.sbri.fr/user/1453

Abstract: Maximum Likelihood Difference Scaling was used to measure suprathreshold contrast response difference scales for low-frequency Gabor patterns modulated along luminance and L-M color directions in normal, protanomalous, and deuteranomalous observers. Based on a signal-detection model, perceptual scale values, parameterized as d', were estimated by maximum likelihood. The difference scales were well fit by a Michaelis-Menten model, permitting estimates of response and contrast gain parameters for each subject. Anomalous observers showed reduced response gain for L-M contrasts, consistent with attenuated chromatic signals from reduced cone separation, but no differences from normal for luminance contrasts. Surprisingly, contrast gain was significantly higher along *both* L-M and luminance axes in anomalous trichromats compared to normals. We consider possible mechanisms that generate these differences in anomalous observers.

1. Introduction

Anomalous trichromacy is classically defined by abnormal shifts in the mixture of reddish and greenish primaries in metameric matches to a yellowish standard [1]. Observers termed protanomalous use more of the reddish primary in the match, and deuteranomalous observers use more of the greenish one. Based on colorimetric [2–5] and genetic [6, 7] studies, it is generally held that the change in matching behavior is explained by shifts in the peaks between the spectral sensitivities of the middle- (M-) or long- (L-) wavelength sensitive cone photoreceptors compared to normal (Fig. 1a). Specifically, deuteranomaly is thought to arise from a substitution of the normal M-cone with a variant L-cone shifted toward longer wavelengths than the normal M-cone [7, 8] and is denoted by L'. Similarly, in protanomaly the normal L-cone photopigment is replaced by a variant M-cone that is shifted toward shorter wavelengths than the normal L-cone and is denoted by M'.

Losses in discrimination that many (but not all [9, 10]) anomalous observers display are attributed to the reduction in the spectral signal from the greater overlap of the cone spectral sensitivities. While there is variation in peak separations for both normal [11] and anomalous observers [10], this loss can be visualized for average observers by plotting the difference in the two long-wavelength spectral sensitivities shown in Fig. 1b [12]. The long-wavelength chromatic difference signal is reduced in anomalous observers with respect to the normal curve. The peak-to-trough difference of the protanomalous curve is 41% of the normal, and that of the deuteranomalous, 25% of the normal. Nevertheless, despite affecting approximately 6% of Caucasian males, little is known about the consequences for color appearance.

In sex-linked anomalous trichromats, red-green hue cancellation showed a relative reduction of chromatic valence that was correlated with anomaloscope matching range [13]. Several studies in

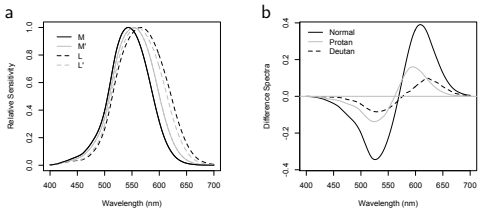

Fig. 1. a. DeMarco, Pokorny and Smith fundamentals [12] for normal M and L cones (black solid and dashed, respectively) and average anomalous observers' M' and L' cone spectral sensitivities (dashed and solid grey, respectively). b. Difference spectra of two long-wavelength sensitive cone spectral sensitivity functions for average normal (black solid), protanomalous (grey solid) and deuteranomalous (black dashed) observers. The weights were chosen so that the net response to an equal-energy light is zero.

which perceived color differences were estimated by multidimensional scaling (MDS) reported compression of perceived differences along the red-green axis, consistent with the reduced chromatic input signal from the greater overlap of cone spectral sensitivities [14–20]. Boehm, MacLeod and Bosten [21], however, found that the compression in the perception of large color differences was much less than that obtained in discrimination experiments. As the discrimination results were well explained by the loss of spectral information at the input, they suggested that a post-receptoral gain amplification occurred in the anomalous observers at suprathreshold levels. Support for post-receptoral gain amplification in anomalous trichromacy has also been reported from functional cerebral imaging [22]. These results fit with a theory proposed by MacLeod that the reduced input signal would be mapped onto the full range of neural response, thereby compensating for the genetic effects on the spectral tuning of photopigment spectra [23, 24].

MacLeod described the consequences of two hypotheses to explain possible adaptations of anomalous observers to their reduced spectral information [23]. If anomalous vision was limited by noise at the input (e.g., at the photoreceptors), then such observers would experience poor discrimination at low chromatic contrasts but good discrimination at high chromatic contrasts. On the other hand, if discrimination was limited by output noise at a post-receptoral stage (e.g., at the color-opponent channels), then discrimination would be enhanced at low chromatic contrasts by increasing the channel gain but at the cost of poorer discrimination for large chromatic contrasts. In fact, Boehm et al. interpret their MDS findings as support for increased gain in post-receptoral channels in anomalous trichromacy. MacLeod [23] cites the well documented evidence of a lack of correlation between midpoint match shifts and ranges of Rayleigh matches [9] as circumstantial evidence to support the latter hypothesis as well as discrimination experiments on his own deuteranomalous vision.

Here, we used Maximum Likelihood Difference Scaling (MLDS), a recently introduced scaling method based on a signal detection model [25–27], to compare the change in appearance of suprathreshold contrasts along luminance and L-M chromatic directions in normal and anomalous observers. The method allows contrast response to be evaluated over nearly the entire range of suprathreshold contrasts, thus, allowing the comparison of normal and anomalous responses at extreme contrast levels.

2. Methods

2.1. Observers

Twenty-seven volunteers (ages 18–49) completed testing. They were recruited through flyers and an online portal. Procedures were explained before any testing, and observers provided written informed consent using a protocol approved by the UC Davis Institutional Review Board. All

observers were compensated for their participation.

Equal numbers of participants were classified as normal (mean age = 26.0 yrs), deuteranomalous (mean age = 26.7 yrs) or protanomalous (mean age = 28.9 yrs) trichromats. All participants were male except for two normal-group females. All observers had normal visual acuity (best corrected to 6/6 or better) and had a negative history of retinal disease and neurological disorders affecting vision.

Color vision classification was based on Rayleigh matches with a Neitz OT anomaloscope and the Cambridge Colour Test administered in trivector mode using a calibrated monitor (Eizo FlexScan T566). Additional confirmation of classifications was based on the F2 Plate test, the Farnsworth Panel D-15 test, and the American Optical Hardy-Rand-Ritter pseudoisochromatic plates, all administered under a lamp equivalent to illuminant C.

2.2. Apparatus, Stimuli and Calibrations

Stimuli were displayed on an Eizo (FlexScan T566) CRT monitor with a 40.3 cm diagonal screen size operating at a resolution of 1280×1024 pixels viewed at a distance of 150 cm. The visual path from viewer to stimuli was surrounded by black light baffles internally coated by non-reflective fabric. Observers were refracted for the test distance using standard trial lenses rather than their habitual spectacles if they were tinted or had anti-reflective coating.

Stimuli were displayed with 10–bit color resolution using custom code written in Python 2.7 utilizing the PsychoPy3 package [28] and integrated development environment. Responses were recorded with a 2–button Bluetooth response pad. The display monitor was gamma corrected and chromatically calibrated using a SpectraScan Spectroradiometer 670 placed 150 cm from the screen and the PsychoPy3 IDE's Monitor Center automated screen calibration tool.

The stimuli were horizontal Gabor patterns defined by the equation

$$f(x, y) = L_0 \left(1 \pm c_\theta \exp\left(-\frac{x^2 + y^2}{2}\right) \sin 2\pi y\right), \tag{1}$$

where L_0 is the mean luminance of the screen, x, y position in degrees, and c_θ the contrast of the carrier signal along the axis θ in color space. The sign of the Gabor term was chosen randomly across trials to generate stimuli varying in phase by 180° in order to minimize local adaptation and afterimages. The stimuli were truncated at 4° diameter (4σ) and were in sine phase so that both the space average luminance and chromaticity did not vary across the stimulus. The carrier spatial frequency was 1 cycle per degree (c/deg) and the pattern was offset from a cross-shaped fixation point. Modulation of Gabor patterns was along a luminance axis ([90,0,1], [elevation, azimuth, maximum contrast] in DKL space) or an L-M axis in the isoluminant plane ([0,0,1] in DKL color space) [29]. A brief warning tone preceded each stimulus presentation of 500 ms duration. The steady background was achromatic (CIE (x, y) = (0.33,0.34); Y = 48.1 cd/m^2) and continuously present.

2.3. Procedures

2.3.1. Preliminary Measurements of Contrast Threshold

Preliminary testing of each individual was conducted to determine a minimum perceived contrast (MPC) for both achromatic luminance modulation and L-M isoluminant stimuli. This was estimated using a two-alternative forced-choice staircase method. Each axis was measured separately with a 5–min dark adaptation period followed by a 3–min re-adaptation period viewing the achromatic background. The Gabor patterns were presented 2.8° above a central $0.5° \times 0.5°$ black fixation cross, and the observer's task was to press one of two buttons to indicate whether the stimulus was detected or not. The contrast of the Gabor patterns was varied in seven logarithmic steps from 0.125 to 0.875 of the monitor's maximum displayable (or nominal) contrast in DKL

colorspace. This was followed by three more series of threshold tests, each with progressively smaller steps to bracket the previous threshold contrasts. The MPC was taken as the minimum contrast detected in the final subset of 28 stimuli with an error of ± 0.016 contrast units.

2.3.2. Suprathreshold Contrast Response Difference Scaling

To compare contrast response of normal and anomalous trichromats, we used MLDS to estimate suprathreshold Contrast Response Difference Scales (CRDS) [25–27]. Gabor patterns, as described above, were modulated along luminance and L-M color directions in DKL color space on a steady achromatic background in an otherwise dark room. On each trial, 3 Gabor patterns ordered in contrast were presented (0.5 sec, 2.8° eccentricity). The middle value contrast was presented 2.8° above the central fixation cross with the other two straddling the same radial distance to the left and right below the fixation cross (Fig. 2). The lateral positions of the lowest and highest contrast were randomized across trials. A forced-choice response indicated whether the pattern in the upper visual field was judged as more similar in contrast to the lower field pattern on the left or the right. The next trial commenced 0.3 sec after the subject's response. For each axis of modulation, a range of 9 contrasts was generated in which the lowest was the

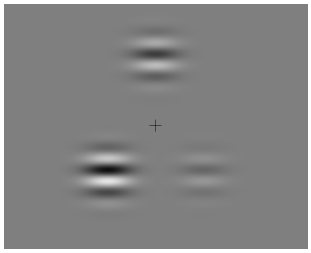

Fig. 2. Three luminance Gabor stimuli from an example difference scaling trial. The observer judges to which of the bottom stimuli the top stimulus appears most similar in contrast.

previously estimated MPC value of the observer, the highest was 90% of the maximum nominal display contrast, and the sequence of contrasts was equally spaced between these extreme values on a logarithmic axis. Observers were able to order the stimuli by contrast. This resulted in 84 forced-choice trials, each preceded by an auditory tone to denote stimulus onset. The order of the contrast triads across trials was random. Each series of 84 trials was completed six times for each axis of stimulus modulation. Rest periods were provided after each series of trials or when a subject requested a break. The rest periods were followed by a 3-min adaptation period to the achromatic background. The two color axes were tested separately. Test runs were distributed over 4 sessions.

2.4. Data Analysis and Modeling

2.4.1. MLDS

All statistical analyses were performed using the OpenSource software R [30]. The signal detection model underlying MLDS and the fitting procedure have been previously described [25–27, 31, 32]. In summary, given a set of p stimuli ordered along a physical continuum, triples or non-overlapping quadruples are sampled on each trial. As we used here the method of triads, we will develop the model in terms of triples. Given a trial with physical triples $\phi(a) < \phi(b) < \phi(c)$, we assume a mapping (not necessarily monotonic) onto internal responses, $\psi(a), \psi(b), \psi(c)$. The observer

considers the noise-perturbed internal decision variable

$$\begin{aligned}\delta(a,b,c) &= (\psi(b)-\psi(a))-(\psi(c)-\psi(b))+\epsilon \\ &= 2\psi(b)-\psi(a)-\psi(c)+\epsilon \\ &= \Delta(a,b,c)+\epsilon,\end{aligned} \tag{2}$$

where we have abbreviated $\phi(a)$ by a, etc. and $\epsilon \sim N(0,\sigma^2)$. The noise perturbation is called the judgment noise and provides for inconsistencies in the observer's responses when the decision variable is sufficiently small. If on a given trial $\delta < 0$, the observer chooses a, otherwise c. We code the observer's responses, R, by 1 or 0 depending on whether the choice is stimulus a or c. From the ensemble of responses to all triads, we compute the log likelihood function for a Bernoulli distributed variable

$$\ell(\Psi;\mathbf{R}) = \sum_{i=1}^{n} R_i \log\left(\Phi\left(\frac{\Delta_i}{2\sigma}\right)\right) + (1-R_i)\log\left(1-\Phi\left(\frac{\Delta_i}{2\sigma}\right)\right), \tag{3}$$

where Φ is the cumulative distribution function for the standard Gaussian, $\mathbf{R}$ is the vector of responses to all triads and Ψ is the vector of scale values, ψ_i. The scale values and judgment noise are chosen as the values that maximize Eq. 3. While it appears that the model requires estimation of $p+1$ parameters, to obtain an identifiable solution, we fix the lowest value at 0 and $\sigma = 1$. This yields $p-1$ scale parameters to estimate corresponding to $\psi_2, \psi_3, \ldots, \psi_p$. The parameterization in Eq. 3 renders the scale values in terms of the signal detection parameter d' since one unit on the response axis corresponds to the standard deviation of the judgment noise. In practice, we fit the data using functions from the R package **MLDS** [26, 27]. These functions implement the fitting procedure in terms of a generalized linear model with a binomial family [26, 27, 31–33]. The obtained scales are unique up to addition of a constant or multiplication by a coefficient. They have the property that stimulus pairs, separated by equal differences on the ordinate, should appear equally different.

2.4.2. Fitting the response scales

Individual CRDSs were found to be well fit by a Michaelis-Menten function offset by the estimated MPC, c_0

$$d'(c) = R_m \frac{c-c_0}{(c-c_0)+\varsigma}, \tag{4}$$

where c is the stimulus contrast, R_m the maximum response, taken as a measure of response gain, and ς the semi-saturation constant, which is reciprocally related to the contrast gain. The effect of the term c_0 is to translate the function along the contrast axis as shown by the dashed curve in Fig. 3. As a result, the value of ς is estimated with respect to the value of c_0. The asymptotic value given by the same value of R_m for both curves is indicated by the dashed grey line.

To compare groups, we fit the data from the three groups of observers with Eq. 4 using a nonlinear mixed-effects model [34].

$$\begin{aligned} d'_o(c) = (R_m + R_t + r_o)\frac{c-c_0}{(c-c_0)+(\varsigma+\varsigma_t+s_o)} + \epsilon_i \\ \epsilon_i \sim N(0,\sigma^2) \\ r_o \sim N(0,\sigma^2_{r_o}) \\ s_o \sim N(0,\sigma^2_{s_o}), \end{aligned} \tag{5}$$

where R_m is the response gain for the normal group, R_t the difference from normal of response gain for the protanomalous or deuteranomalous group, ς the semi-saturation constant for the

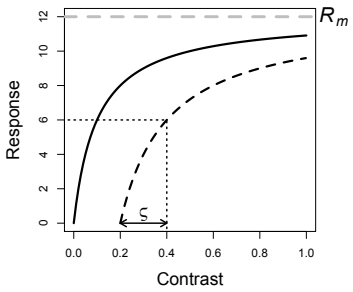

Fig. 3. Michaelis-Menten function plotted as a function of contrast with the initial value at zero (solid) and with the minimum contrast translated to 0.2 (dashed). In the translated version, ς is estimated with respect to the translated origin. In both cases the maximum asymptotic value is the same, as shown by the grey dashed line.

normal group, and ς_t, the difference from normal for the protanomalous or deuteranomalous group. The model includes two random effects in addition to the independently and identically distributed mean-zero standard Gaussian random variation across scale values, ϵ: random effects of response gain across observer r_o and of the semi-saturation constant across observer, s_o, each assumed to be mean-zero Gaussian distributed with variances $\sigma^2_{r_o}$ and $\sigma^2_{s_o}$, respectively. The difference of response and contrast gain of the anomalous observers from normal was evaluated by assessing whether the terms R_t and ς_t differed from zero. This was accomplished by evaluating Eq. 5 with respect to the nested model in which these terms were fixed at zero using a likelihood ratio test. Data obtained along luminance and L-M axes were fit in separate analyses.

3. Results

Figure 4 shows estimated CRDSs for example individual normal (a, d), protanomalous (b, e) and deuteranomalous (c, f) observers. The results from observers classified with the same type of color vision were qualitatively similar and are displayed in the Appendix (Fig. A1) and Supplementary Figs. S1–3 (all supplementary figures and tables referred to in this article can be downloaded from https://www.sbri.fr/sites/default/files/supplementary.pdf). Response scales for luminance contrast stimuli are indicated as filled points and L-M as unfilled points in Fig. 4. The points indicate averages of data collected from sessions on the same day. The curves are the nonlinear least-squares Michaelis-Menten fits which describe the data well in all conditions. The estimated parameters to reproduce each of the individual curves are provided in Supplementary Tabs. S1–2, for data collected for contrasts along the luminance and L-M axes, respectively. Standard errors indicated below and in the Supplementary tables were obtained from the variance-covariance matrix at the maximum likelihood. In order to perform the fits, the data from different days were shifted vertically to minimize the vertical distances between data sets, as such a transformation has no effect on the predicted responses. The shifts required were always small, less than 1% of the response range. On the top row, the data are plotted in nominal contrast with a value of 1.0 corresponding to the maximum output of the display. The estimated MPC for the two anomalous observers is slightly higher than the value for the normal along the luminance axis (N: 0.008; P: 0.016; D: 0.023), but it is much higher than the normal for the anomalous observers along the L-M axis (N: 0.037; P: 0.121; D: 0.351). The estimated luminance R_m values (± 1 standard error) were similar for the three observers (N: 10.5 ± 0.53; P: 10.4 ± 0.35, D: 11.9 ± 0.49), but the L-M values were systematically lower for the anomalous observers (N: 6.9 ± 0.42; P: 4.7 ± 0.14; D: 3.4 ± 0.16).

For anomalous observers, the initial branch of the curves appears to rise more steeply to an asymptotic value than for the normal observers. This is confirmed by the ς estimates that were lower along both luminance and L-M axes for the anomalous observers (Luminance: N: 0.21 ± 0.027; P: 0.09 ± 0.010; D: 0.11 ± 0.014; L-M: N: 0.22 ± 0.032; P: 0.10 ± 0.009; D: 0.10 ± 0.012). The steep rise for anomalous observers is more clearly displayed in the bottom set of graphs in which the same data for each observer have been replotted in terms of cone contrasts and the abscissa is logarithmically scaled. Using the DeMarco, Pokorny and Smith cone spectral sensitivities for average observers with each color vision type [12], the maximum L-M cone contrasts that could be displayed were estimated as: Normal 0.142, Protanomalous 0.037, and Deuteranomalous 0.041. These values were used to rescale the L-M contrasts in the bottom row of graphs. In cone contrast units, all observers responded to the L-M gratings at lower contrasts than the luminance gratings [35]. However, with the adjustment to cone contrasts the MPC values along the L-M axis for all three groups of observers converged toward similar values.

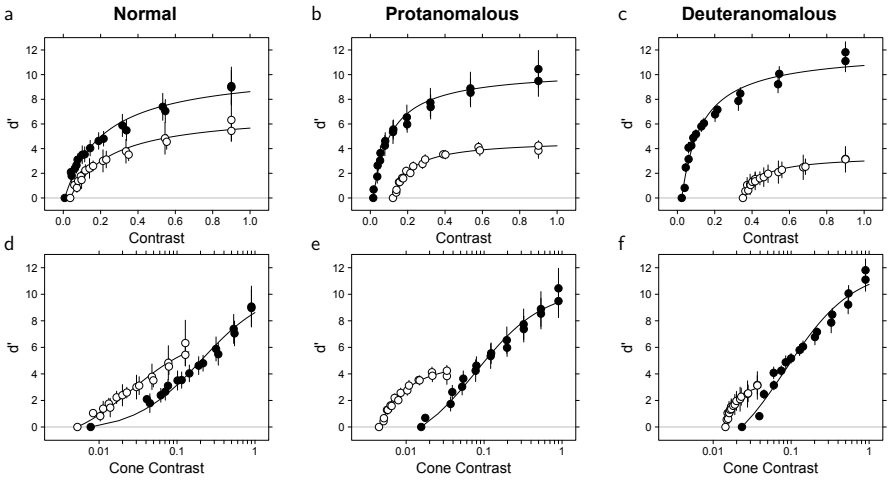

Fig. 4. CRDSs estimated by MLDS measured along the luminance (filled symbols) and L-M (unfilled symbols) axes. The top row (a, b, c) shows data from individual normal (N1), protanomalous (P4) and deuteranomalous (D1) observers plotted in nominal contrast units. The bottom row (d, e, f) shows the same data from the respective observers replotted as a function of cone contrast with a logarithmically spaced abscissa for clarity of presentation. The solid curves are Michaelis-Menton functions best-fit by nonlinear least squares. The error bars are 95% confidence intervals.

Figure 5a shows the MPC values in nominal contrast for the three classes of observer along both axes tested. To homogenize the variance, a 2-way analysis of variance (ANOVA) was performed on the log(MPC), with factors color vision type and color axis tested. The interaction was significant ($F(4,48) = 8.1751$, $p \ll 0.001$) indicating that the relative dependence of the MPC on color vision type differed between the two axes tested (Supplementary Tab. S3). Examination of the model coefficients provided no evidence of differences between anomalous and normal observers along the luminance axis (P vs N: $t(48) = 0.22$, $p = 0.83$; D vs N: $t(48) = -0.09$, $p = 0.93$) but strong evidence for a difference along the L-M axis (P vs N: $t(48) = 4.4$, $p \ll 0.001$; D vs N: $t(48) = 5.37$, $p \ll 0.001$) (Supplementary Tab. S4). The black triangles plotted with the anomalous data in the L-M plot indicate the expected reduction in sensitivity with respect to the mean normal MPC due to the relative peak-to-trough reduction of the L-M functions because of the reduced spectral separation of the photopigments (Fig. 1b).

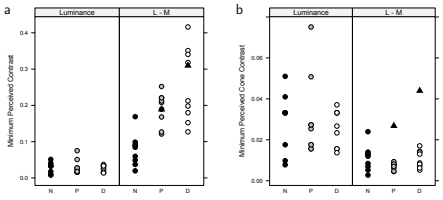

Fig. 5. a. Individual estimates of the MPC in nominal contrast units for normal (N), protanomalous (P) and deuteranomalous (D) observers along luminance and L-M axes. The black triangles on the L-M plot for protan and deutan observers correspond to the reduction of the mean normal MPC expected from the reduced separation of the cone spectral sensitivities. b. Individual estimates of MPC adjusted in units of cone contrast for the 3 classes of observers and both axes of color space.

When the MPC values are expressed as cone contrasts (Fig. 5b), however, the values along the L-M values no longer differ among groups as indicated by a one-way ANOVA ($F(2, 24) = 1.5$, $p = 0.24$) (Supplementary Tab. S5). We did not re-analyze the luminance values because these are unchanged in terms of cone contrasts. The results support the hypothesis that at the level of cone contrasts, all observers require similar signals to perceive a minimal contrast [36]. The calculation of the cone contrasts with the anomalous fundamentals takes account of the reduced spectral distances between the cone sensitivities so that the black triangles that correct for this information loss with respect to the normal no longer fall within the anomalous distributions of values.

We fit the Michaelis-Menten function to the data of all observers using a nonlinear mixed-effects model [34], as specified in Eq. 5. Equation 4 was used as the fixed-effect component. An observer-dependent random effect was attributed to both R_m and ς, each assumed to be normally distributed with its own variance term. The constant c_0 was not estimated, and the individual MPC values were used. Analyzing the data from luminance and L-M directions together revealed inhomogeneity in variance across the two conditions. Therefore, the data from each axis were analyzed separately.

The scales of the two parameters R_m and ς differed by a factor of 50, so it would be misleading to compare the variance accounted for by each random effect. The coefficient of variation (cv) is a more informative statistic and is given by the ratio of the square root of the variance component to the mean value and indicates the proportional variation across observers. Along the luminance axis, the cv for R_m was 0.145 and for ς was 0.199. Along the L-M axis, the cv for R_m was 0.207 and for ς it was 0.381 (Supplementary Tabs. S7 and S15).

Figure 6a shows the fixed-effect or population estimates for the CRDSs for the luminance axis for the three observer classes. The upper asymptote is similar for normal and protanomalous observers but is slightly elevated for the deuteranomalous (Fig. 7a, Supplementary Tab. S6). A likelihood ratio test, however, comparing models in which R_m could vary among the three groups with the nested model in which R_m was constrained to be the same across groups, yielded no evidence for a significant difference ($\chi^2(2) = 1.01, p = 0.60$) (Supplementary Tab. S10). The anomalous curves appear to rise a little more steeply, suggesting a higher contrast gain for luminance contrasts for these observers (Fig. 7b, Supplementary Tab. S6). A nested likelihood ratio test, in which the nested model fixed ς across groups, provided convincing evidence for a difference among the values ($\chi^2(2) = 9.59, p = 0.008$) (Supplementary Tab. S13). A test on the individual values supported the hypothesis that the anomalous values differed from the normal (P vs N: t(429) = -2.93; p = 0.004; D vs N: t(429) = -3.15, p = 0.002) (Supplementary Tab. S8).

Figure 6b shows the population curves for the L-M axis in nominal contrast units. The curves for the anomalous observers asymptote at lower values (Fig. 7a) and rise more steeply (Fig. 7b)

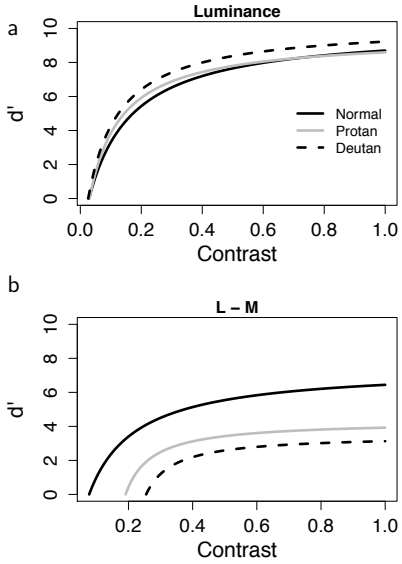

Fig. 6. a. Population estimates from nonlinear mixed-effects model for luminance CRDS of normal (solid black), protanomalous (solid grey) and deuteranomalous (dashed black) observers. b. Population estimates from nonlinear mixed-effects model for L-M CRDS in nominal contrast units for the three classes of observers using the same color coding as in a.

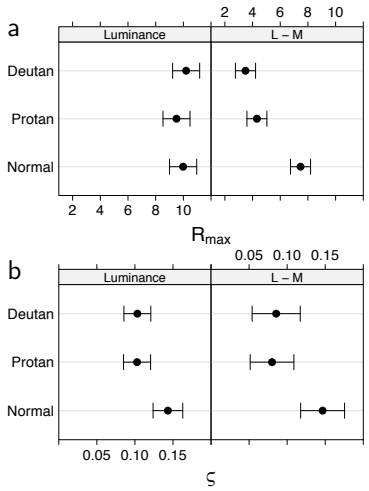

Fig. 7. a. Population mean and 95% confidence intervals of the response gain parameter, R_m for normal and anomalous trichromatic observers for CRDSs measured along the luminance and L-M axes. b. Population mean and 95% confidence intervals of the semi-saturation parameter, ς for normal and anomalous trichromatic observers for CRDSs measured along the luminance and L-M axes.

than the normal curve (Supplementary Tab. S14). Nested likelihood ratio tests confirmed the differences both for R_m ($\chi^2(2) = 33.2$, $p \ll 0.001$) (Supplementary Tab. S18) and for ς ($\chi^2(2) =$

8.4, p = 0.02) (Supplementary Tab. S21). The differences in contrast gain along the L-M axis cannot be accounted for by the expression of the contrasts in nominal units as the transformation to cone contrasts only exaggerates the difference in anomalous ς values from normals (N: 0.021; P: 0.003; D: 0.004).

4. Discussion

4.1. MLDS

We have demonstrated that MLDS is an effective method for obtaining estimates of the change in appearance of Gabor patterns over a contrast range not accessible with threshold measures of contrast sensitivity. Figure 8 shows a psychometric function for luminance contrast detection (dashed curve) based on the ModelFest data set [37] for estimating threshold of a Gabor stimulus at 1 c/deg using a Weibull function. The solid curve replots the normal luminance MLDS population curve from Fig. 6a. It is notable that there is no stimulus range overlap between the increasing sections of each function. The psychometric function yields information at low contrast values over a four-fold range, whereas the MLDS curve yields information over suprathreshold contrast values spanning a thirty-fold range.

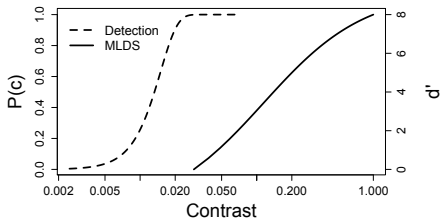

Fig. 8. Comparison of contrast, c, ranges over which the psychometric function for luminance contrast detection and MLDS scaling operate. The psychometric function (dashed curve and left ordinate values) is a Weibull function, $1 - \exp\left(-\left(\frac{c}{\alpha}\right)^{\beta}\right)$, with threshold, α based on an estimation of the threshold of a 1 c/deg luminance Gabor function from the ModelFest data set [37] with $\beta = 3$. The MLDS function (solid curve and right ordinate values) represents the normal population luminance CRDS replotted from Fig. 6a.

The method that we describe is efficient. For 9 contrast levels, as used here, that result in an 84-trial session, an experienced observer can typically complete the full set of trials in 2–3 min with data that yield a relatively accurate estimation of the curve. Naive observers require practice sessions to understand the task and stabilize their criteria and generally require longer to complete a session. In both cases, repeated sessions lead to more precise estimates of the curve shape and the fitted parameters.

Contrast response can also be estimated with pedestal experiments. These require estimating a discrimination threshold at each contrast level tested, and the underlying response function is indirectly estimated based on the hypothesis that size of the discrimination threshold is inversely proportional to the underlying response. Such estimates have yielded a slightly more complex functional form to describe the contrast response function in which each term in the numerator and the denominator of the Michaelis-Menten function is raised to a positive exponent [38]. This yields an accelerating response function at low contrasts and a compressive one at high. We found that we could fit our data well assuming that such an exponent is equal to unity. The suprathreshold levels at which MLDS is conducted may not cover the range over which an accelerating nonlinearity is necessary to describe contrast response.

The representation of the MLDS response scale in terms of the signal detection parameter d' is based on a parameterization that sets the judgment noise equal to unity on the response scale. How this measure of d' relates to that obtained from discrimination experiments is an unsettled question [31, 32] that perhaps can be answered by comparing MLDS response estimates directly with those from discrimination experiments.

Finally, we propose that this approach could be valuable in assessing visual function in pathology of visual pathways. While patients will likely be more challenging to test than observers with normal vision, it would be of interest to identify conditions that differentially influence response and contrast gain. For example, a previous study used MLDS to scale contrast appearance for square-wave, radial checkerboards and correlated the scales to responses generated using functional cerebral imagery with respect to cortical area V1 and sub-cortical areas LGN and superior colliculus in each of three age groups [39]. As in the current study, these results were well described by Eq. 4. Analyses of the response and contrast gain parameters indicated significant decreases in response gain and increases in contrast gain with age.

4.2. MPC

The stimulus levels used in an MLDS experiment must be above threshold and, in principle, the observer should be capable of sorting them in order [25]. Thus, to obtain measures over the widest contrast range for each observer, we estimated a minimal contrast that could be reliably perceived that we termed the MPC.

We observed that the MPC did not differ significantly among normal and anomalous observers along the luminance axis. Thus, we do not confirm a recent study reporting that anomalous observers display higher luminance contrast sensitivity than normal observers [40]. This may reflect that MPC does not, strictly speaking, correspond to a measure of contrast threshold as we did find that anomalous observers displayed enhanced contrast gain (Fig. 7a) as discussed in Sect. 4.4 below.

Expressed in the nominal display contrasts, the L-M MPC of anomalous observers was on average almost three times higher than that of normal observers. This is consistent with the reduced peak-to-trough reduction in chromatic difference signals at the input described in Sect. 1 and in agreement with the findings of Boehm et al. [21] with respect to chromatic discrimination loss in anomalous observers. Nevertheless, when expressed as cone contrasts using average cone fundamentals for normal and anomalous observers, the values converged for all three classes of observers. This supports the hypothesis that normal and anomalous observers require similar response differences to perceive contrast at the physiological level, and is consistent with the analyses of Pokorny and Smith [36] that show that anomalous discrimination can be mapped onto normal discrimination over a reduced stimulus range.

4.3. Contrast Appearance along the L-M Axis

Along the L-M axis, anomalous observers showed reduced response gain and increased contrast gain with respect to normal observers (Fig. 7). R_m values were, on average, 52% of normal while ς values were 57% of the normal value. The reduction in response gain is less than that predicted due to amplitude reduction of the L-M response shown in Fig. 1b (41% and 25% for protan and deutan observers, respectively) in support of a compensatory post-receptoral amplification gain.

The value of ς is taken to be inversely proportional to contrast gain, so we should be considering its reciprocal. In these units, the anomalous contrast gains were on average 1.8 times larger than the normal values. Corrected to cone contrasts, the average gain increase was greater than a factor of 6. This is most easily observed in the steeper rise of d' along the contrast axis in Fig. 7b. The curves predict that at contrasts just above threshold, anomalous observers should show enhanced contrast discrimination along the L-M axis. At high contrasts the curves flatten out, indicating that contrast discrimination should become worse, perhaps even showing saturating behavior as

in rod discrimination at high luminance levels [41]. These results support MacLeod's prediction of response in the presence of output noise and Boehm et al.'s conclusions of a post-receptoral gain amplification [21].

4.4. Contrast Appearance along the Luminance Axis

Surprisingly, the results indicated that contrast gains were also significantly greater in anomalous than normal trichromats for luminance contrasts (Fig. 7b). Even though there is no difference in the response gain for the normal and anomalous observers, the initial section of the contrast response curves rises more steeply for both classes of anomalous than in the normal sample (Fig. 6b). These results lead to the prediction that anomalous observers would, on average, show superior luminance contrast discrimination at low contrasts up to ~0.2 in accord with a recent report that anomalous observers display enhanced contrast sensitivity with respect to normal observers [40].

This could be explained if the gain amplification occurs at a site in common with the mechanisms mediating responses to stimuli along both the luminance and L-M axes. Several possibilities exist for such a mechanism. Neurons in the parvocellular pathway have single-opponent receptive fields with different spectral sensitivities in the center and surround [42–44]. In this way, they transmit both luminance and chromatic information. The long duration of the stimulus presentations (0.5 sec) does not preclude the possibility of participation of neurons in the parvocellular pathway, even though the spatial frequency of the stimuli was relatively low (1 c/deg). At the cortex, the most prevalent cell type responsive to color has an orientation-selective, double-opponent receptive field that is tuned along both chromatic and luminance axes [45]. A less parsimonious hypothesis would be that the gain amplification in response to the reduced chromatic input promiscuously influences independent luminance and chromatic pathways.

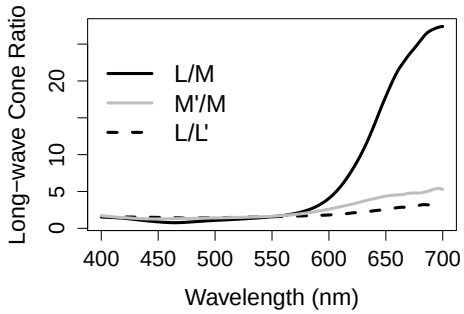

Fig. 9. Ratio of average long- to middle-wavelength sensitive cone spectral sensitivities in normal (black solid), protanomalous (grey) and deuternanomalous (black dashed) observers weighted by average normal cone ratios.

Alternatively, the increased luminance contrast gain in anomalous observers is due to a different mechanism than that hypothesized for L-M contrasts. In normal observers, it has been argued that luminance is mediated by neurons in the magnocellular pathway [46]. This pathway begins with the retinal parasol cells. Since these cells sample indiscriminately from M and L cones, individual luminance spectral sensitivities based on heterochromatic flicker photometry in normal observers can be described by a linear combination of L and M cone responses with the weights reflecting the relative numbers of L and M cones in the retinal region sampled [47]. In average retinas, this yields an L/M ratio of about 1.6, based on the fit of the normal M and L cones to V_λ. Figure 9 shows that the consequence of this is that the L cones dominate the expected normal LM ratio at long wavelengths (solid black). In anomalous trichromats, however, the reduced separation of the two long-wavelength spectral sensitivities results in a more nearly equal

contribution from each cone class.

We hypothesize that this imbalance of contributions in the normal retina results in an effective reduction of the number of receptor samples contributing to luminance with respect to anomalous observers, or conversely, an increase in the effective number of samples in anomalous observers. In principle, an increased number of samples will reduce noise, which would lead to increased sensitivity to contrast, reflected in an increased contrast gain. In the limiting case for equal numbers of both long-wavelength cone classes, the maximum increase in gain would be expected to be the square root of 2. The average ratio observed in our data is 1.39 with 95% confidence interval (1.09, 1.70), which includes the expected ratio of 1.25, given the average ratio of L to M cones cited above, but is sufficiently large not to exclude any particular hypothesis. This sampling hypothesis, however, would predict a similarly increased contrast gain in dichromatic observers for luminance contrasts while the hypothesis that the gain reflects a common mechanism operating along the two axes in color space does not, since, in theory, there is no L-M signal in the dichromatic visual system for which to amplify the gain.

Doron et al. [40] predict and provide evidence that anomalous observers have enhanced performance in detecting objects in camouflage, beyond what would be expected from any differences from the normal in metamerism. Under the sampling hypothesis stated above, a similar advantage would be expected for dichromats, and, in fact, has previously been reported [48]. In any case, if an increased contrast gain leads to an advantage in camouflage detection, given the increased contrast gains found along the L-M axis in anomalous trichromats, we would predict them to also display a similar advantage for color contrasts.

4.5. Implications for Compensation

Our results suggest a plasticity in visual system organization that optimizes the mapping between stimuli and neural response [23, 24]. Observers with anomalous trichromacy displayed higher contrast gain along a chromatic axis in color space despite a reduced chromatic signal at the input. In the case of these observers, the loss of signal is congenital. There is considerable evidence, however, for dynamic changes to the input in normal sensory systems. For example, Kwon et al. [49] exposed normal observers to contrast reduced environments for several hours and observed enhancements in contrast discrimination psychophysically and in neural responses in cortical areas V1 and V2 measured with functional cerebral imagery. Unlike the current results, the model that best described their data required a change in response gain alone and no change in contrast gain.

It has previously been suggested that the loss of chromatic signal in anomalous trichromats due to reduced separation of the cone spectral sensitivities might be ameliorated by the use of selective filters that would act to increase their spectral separation [50, 51]. The MLDS paradigm for measuring contrast appearance would be an ideal paradigm for studying the long-term effects of such aids on contrast perception.

5. Conclusion

Contrast response as estimated with a maximum likelihood scaling method is well described by a Michaelis-Menten function. The minimum suprathreshold contrast estimated for using the MLDS method was similar for normal and anomalous trichromats along both the luminance and L-M axes when expressed as cone contrast, suggesting that the neural requirements for detecting contrast are the same for both sets of observers. Anomalous trichromats display a reduced response gain along the L-M axis but do not differ from normal trichromats for luminance contrast. Anomalous trichromats display higher contrast gain along both luminance and L-M axes. It is proposed that the L-M enhancement in contrast gain is due to a post-receptoral gain amplification while the luminance enhancement is consistent with an effective increase in photoreceptor sampling rate in anomalous trichromats arising from the reduced separation of

their long-wavelength cone spectral sensitivities that in turn increases sensitivity via reduced sampling noise.

Appendix

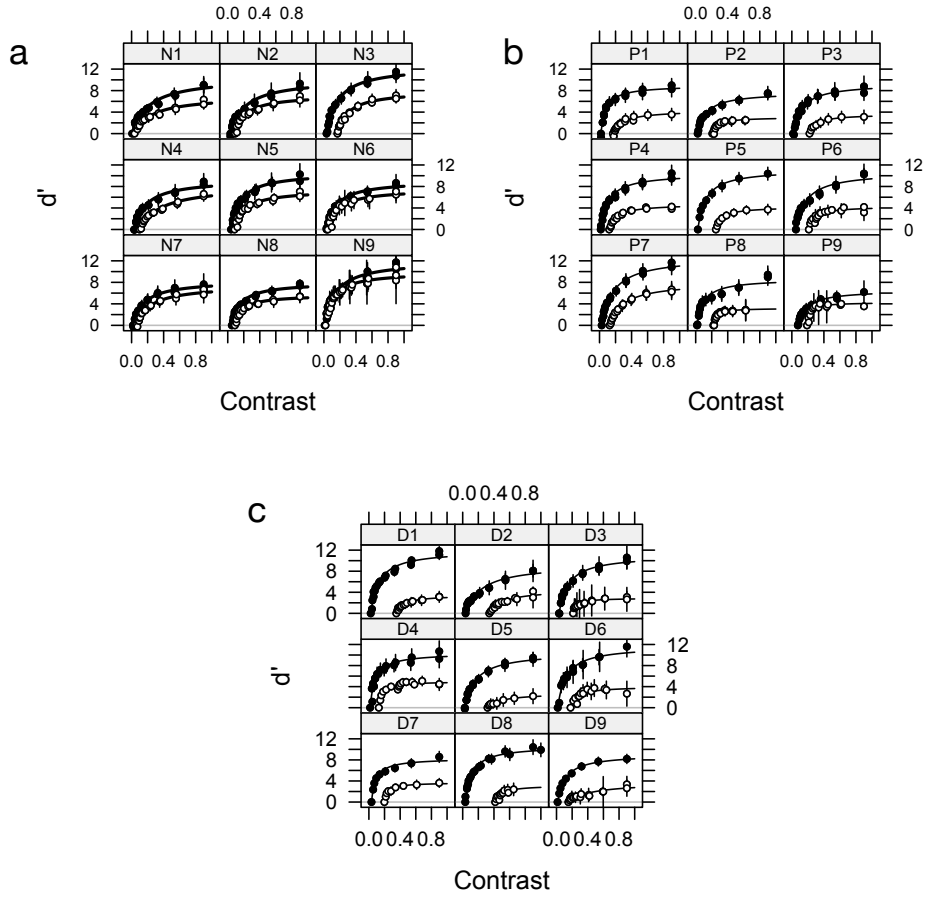

Fig. A1. CRDSs parameterized in terms of d' for all individual observers on a nominal contrast scale, where the maximum contrast value corresponds to the maximum attainable contrast on the display. The black symbols are for measurements along the luminance axis and the while along the L-M axis. The curves are the best-fit Michaelis-Menten functions by a least-squares method. a. Normal, b. Protanomalous, c. Deuteranomalous

Funding

KK was supported by the following grants: LABEX CORTEX (ANR-11-LABX-0042) of Université de Lyon (ANR-11-IDEX-0007) operated by the French National Research Agency (ANR), ANR-11-BSV4-501, CORE-NETS, ANR-14-CE13-0033, ARCHI-CORE, ANR-15-CE32-0016, CORNET, ANR-17- NEUC-0004, A2P2MC, ANR-17-HBPR-0003, CORTICITY. JSW and BMA were supported by the National Eye Institute (R01 EY 024239).

Acknowledgments

We thank Susan Garcia for assistance in subject screening and testing.

Disclosures

The authors declare no conflicts of interest.

References

1. J. Strutt, "Experiments on colour," Nature **25**, 64–66 (1881).
2. W. M. McKeon and W. Wright, "The characteristics of protanomalous vision," Proc. Phys. Soc. **52**, 464 (1940).
3. W. Rushton, D. S. Powell, and K. White, "Pigments in anomalous trichromats," Vis. Res. **13**, 2017–2031 (1973).
4. J. Pokorny, V. C. Smith, and I. Katz, "Derivation of the photopigment absorption spectra in anomalous trichromats," J Opt Soc Am **63**, 232–237 (1973).
5. S. K. Shevell and J. C. He, "The visual photopigments of simple deuteranomalous trichromats inferred from color matching," Vis. Res. **37**, 1115–1127 (1997).
6. J. Nathans, T. P. Piantanida, R. L. Eddy, T. B. Shows, and D. S. Hogness, "Molecular genetics of inherited variation in human color vision," Science **232**, 203–210 (1986).
7. S. L. Merbs and J. Nathans, "Absorption spectra of the hybrid pigments responsible for anomalous color vision," Science **258**, 464–466 (1992).
8. M. Alpern and J. Moeller, "The red and green cone visual pigments of deuteranomalous trichromacy." The J. Physiol. **266**, 647–675 (1977).
9. L. M. Hurvich, "Color vision deficiencies," in *Visual Psychophysics,* (Springer, 1972), pp. 582–624.
10. D. Jameson, L. Hurvich, and D. Varner, "Discrimination mechanisms in color deficient systems," in *Doc. Ophthal. Proc. Ser.*, vol. 33 (1982), pp. 295–301.
11. M. A. Webster and D. I. MacLeod, "Factors underlying individual differences in the color matches of normal observers," J Opt Soc Am A Opt Image Sci Vis **5**, 1722–1735 (1988).
12. P. DeMarco, J. Pokorny, and V. C. Smith, "Full-spectrum cone sensitivity functions for X-chromosome-linked anomalous trichromats," J Opt Soc Am A Opt Image Sci Vis **9**, 1465–1476 (1992).
13. M. Romeskie, "Chromatic opponent-response functions of anomalous trichromats," Vis. Res. **18**, 1521–1532 (1978).
14. M. Müller, C. Cavonius, and J. Mollon, "Constructing the color space of the deuteranomalous observer," in *Colour Vision Deficiencies X,* (Springer, 1991), pp. 377–387.
15. B. Regan and J. Mollon, "The relative salience of the cardinal axes of colour space in normal and anomalous trichromats," in *Colour Vision Deficiencies XIII,* (Springer, 1997), pp. 261–270.
16. G. Paramei, C. A. Izmailov, and E. Sokolov, "Multidimensional scaling of large chromatic differences by normal and color-deficient subjects," Psychol. Sci. **2**, 244–249 (1991).
17. G. V. Paramei, "Color space of normally sighted and color-deficient observers reconstructed from color naming," Psychol. Sci. **7**, 311–317 (1996).
18. G. V. Paramei and C. R. Cavonius, "Color spaces of color-normal and color-abnormal observers reconstructed from response times and dissimilarity ratings," Percept. & Psychophys. **61**, 1662–1674 (1999).
19. G. V. Paramei, D. L. Bimler, and C. R. Cavonius, "Color-vision variations represented in an individual-difference vector chart," Color. Res. & Appl. **26**, S230–S234 (2001).
20. J. M. Bosten, J. D. Robinson, G. Jordan, and J. D. Mollon, "Multidimensional scaling reveals a color dimension unique to 'color-deficient' observers," Curr. Biol. **15**, R950–952 (2005).
21. A. E. Boehm, D. I. MacLeod, and J. M. Bosten, "Compensation for red-green contrast loss in anomalous trichromats," J Vis **14**, 19 (2014).
22. K. E. Tregillus, "Color perception in anomalous trichromats: Neuroimaging investigations of neural compensation for losses in spectral sensitivity," Ph.D. thesis, University of Nevada, Reno (2017).
23. D. I. MacLeod, "The Verriest Lecture. Colour discrimination, colour constancy and natural scene statistics," in *Normal and Defective Colour Vision,* J. Mollon, J. Pokorny, and K. Knoblauch, eds. (Oxford University Press, 2003), pp. 189–217.
24. T. Twer and D. I. MacLeod, "Optimal nonlinear codes for the perception of natural colours," Network: Comput. Neural Syst. **12**, 395–407 (2001).
25. L. T. Maloney and J. N. Yang, "Maximum likelihood difference scaling," J Vis **3**, 573–585 (2003).
26. K. Knoblauch and L. T. Maloney, "MLDS: Maximum likelihood difference scaling in R," J. Stat. Softw. **25**, 1–26 (2008).
27. K. Knoblauch and L. T. Maloney, *Modeling Psychophysical Data in R*, vol. 32 (Springer Science & Business Media, 2012).
28. J. Peirce, J. R. Gray, S. Simpson, M. MacAskill, R. Höchenberger, H. Sogo, E. Kastman, and J. K. Lindeløv, "Psychopy2: Experiments in behavior made easy," Behav. Res. Methods **51**, 195–203 (2019).
29. A. M. Derrington, J. Krauskopf, and P. Lennie, "Chromatic mechanisms in lateral geniculate nucleus of macaque," J. Physiol. (Lond.) **357**, 241–265 (1984).

30. R Core Team, *R: A Language and Environment for Statistical Computing*, R Foundation for Statistical Computing, Vienna, Austria (2019).
31. F. Devinck and K. Knoblauch, "A common signal detection model accounts for both perception and discrimination of the watercolor effect," J Vis **12** (2012).
32. C. B. Wiebel, G. Aguilar, and M. Maertens, "Maximum likelihood difference scales represent perceptual magnitudes and predict appearance matches," J. Vis. **17**, 1–1 (2017).
33. C. Charrier, L. T. Maloney, H. Cherifi, and K. Knoblauch, "Maximum likelihood difference scaling of image quality in compression-degraded images," J Opt Soc Am A Opt Image Sci Vis **24**, 3418–3426 (2007).
34. J. Pinheiro, D. Bates, S. DebRoy, D. Sarkar, and R Core Team, *nlme: Linear and Nonlinear Mixed Effects Models* (2019). R package version 3.1-141.
35. A. Chaparro, E. Huang, R. Kronauer, R. T. Eskew *et al.*, "Colour is what the eye sees best," Nature **361**, 348 (1993).
36. J. Pokorny and V. C. Smith, "Evaluation of single-pigment shift model of anomalous trichromacy," J Opt Soc Am A Opt Image Sci Vis **67**, 1196–1209 (1977).
37. A. B. Watson and A. J. Ahumada, "A standard model for foveal detection of spatial contrast," J. Vis. **5**, 6–6 (2005).
38. G. E. Legge and J. M. Foley, "Contrast masking in human vision," J Opt Soc Am A Opt Image Sci Vis **70**, 1458–1471 (1980).
39. E. Bellot, V. Coizet, J. Warnking, K. Knoblauch, E. Moro, and M. Dojat, "Effects of aging on low luminance contrast processing in humans," NeuroImage **139**, 415–426 (2016).
40. R. Doron, A. Sterkin, M. Fried, O. Yehezkel, M. Lev, M. Belkin, M. Rosner, A. S. Solomon, Y. Mandel, and U. Polat, "Spatial visual function in anomalous trichromats: Is less more?" PloS one **14**, e0209662 (2019).
41. M. Aguilar and W. Stiles, "Saturation of the rod mechanism of the retina at high levels of stimulation," Opt. Acta: Int. J. Opt. **1**, 59–65 (1954).
42. T. N. Wiesel and D. H. Hubel, "Spatial and chromatic interactions in the lateral geniculate body of the rhesus monkey." J. Neurophysiol. **29**, 1115–1156 (1966).
43. R. L. De Valois and P. L. Pease, "Contours and contrast: responses of monkey lateral geniculate nucleus cells to luminance and color figures," Science **171**, 694–696 (1971).
44. C. R. Ingling and E. Martinez-Uriegas, "The relationship between spectral sensitivity and spatial sensitivity for the primate r-g X-channel," Vis. Res. **23**, 1495–1500 (1983).
45. E. Johnson, M. Hawken, and R. Shapley, "The spatial transformation of color in the primary visual cortex of the macaque monkey." Nat Neurosci **4**, 409–416 (2001).
46. B. Lee, P. Martin, and A. Valberg, "The physiological basis of heterochromatic flicker photometry demonstrated in the ganglion cells of the macaque retina." The J. Physiol. **404**, 323–347 (1988).
47. D. H. Brainard, A. Roorda, Y. Yamauchi, J. B. Calderone, A. Metha, M. Neitz, J. Neitz, D. R. Williams, and G. H. Jacobs, "Functional consequences of the relative numbers of L and M cones," J Opt Soc Am A Opt Image Sci Vis **17**, 607–614 (2000).
48. M. J. Morgan, A. Adam, and J. D. Mollon, "Dichromats detect colour-camouflaged objects that are not detected by trichromats," Proc. Royal Soc. London. Ser. B: Biol. Sci. **248**, 291–295 (1992).
49. M. Kwon, G. E. Legge, F. Fang, A. M. Cheong, and S. He, "Adaptive changes in visual cortex following prolonged contrast reduction," J Vis **9**, 1–16 (2009).
50. K. Knoblauch and M. J. McMahon, "Discrimination of binocular color mixtures in dichromacy: evaluation of the Maxwell–Cornsweet conjecture," J Opt Soc Am A Opt Image Sci Vis **12**, 2219–2229 (1995).
51. E. W. Dees and R. C. Baraas, "Fargede filtre gir ikke rød-grønne fargesvake normal fargebedømmelse," Scand. J. Optom. Vis. Sci. **4**, 6–13 (2011).